energy&fuels

Article

pubs.acs.org/EF

Assessing Biodegradation in the Llanos Orientales Crude Oils by Electrospray Ionization Ultrahigh Resolution and Accuracy Fourier Transform Mass Spectrometry and Chemometric Analysis

Boniek G. Vaz,*[,†,‡] Renzo C. Silva,*[,§] Clécio F. Klitzke,[†] Rosineide C. Simas,[†] Heliara D. Lopes Nascimento,[†] Rosana C. L. Pereira,[†,∥] Diego F. Garcia,[⊥] Marcos N. Eberlin,*[,†] and Débora A. Azevedo*[,§]

[†]Laboratório ThoMSon de Espectrometria de Massas, Universidade Estadual de Campinas, Instituto de Química, Campinas, SP, 13083-970, Brazil

[‡]Universidade Federal de Goiás, Instituto de Química, Campus Samambaia, Goiânia, GO, 74001-970, Brazil

[§]Universidade Federal do Rio de Janeiro, Instituto de Química, Ilha do Fundão, Rio de Janeiro, RJ, 21949-900, Brazil

[∥]Petroleo Brasileiro S/A – Petrobras, CENPES, Rio de Janeiro, RJ, 21941-901, Brazil

[⊥]Instituto Colombiano del Petróleo, ICP/ECOPETROL, Bucaramanga, Colombia

ABSTRACT: Focusing on the O_2 class, a set of crude oils from Llanos Orientales Basin, Colombia, were classified in terms of biodegradation levels using negative ion mode electrospray Fourier transform ion cyclotron resonance mass spectrometry (FT-ICR MS) and chemometric analysis. The O_2 class, which is mainly composed of naphthenic carboxylic acids, was monitored because these polar crude oil constituents are known to be substantially affected by microbial activity. Principal component analysis (PCA) applied on the O_2 profile was able to classify the crude oils into three groups: biodegraded, mixture, and non-biodegraded. From the relative abundances of the O_2 class, a clear trend on acid distribution could be directly correlated with biodegradation: a rising in abundance of saturated acids with low double-bond equivalent (DBE) values (despite the lowering observed for fatty acids with DBE = 1), expressed by the A/C index. The combined use of two indexes, the A/C index and a new index also based on saturated acid abundances, the SA index, is proposed as an effective strategy to monitor biodegradation. This approach showed to be particularly useful to fill blanks on discrete biodegradation classification and when samples are actually composed of a mixture of oils with contrasting biodegradation levels. Results are in good agreement with predictions based on classical hydrocarbon biomarker analysis.

INTRODUCTION

Mass spectrometry developments have been historically linked in several occasions to the enormous analytical challenges encountered in the oil industry.[1] Major advances in petroleum analysis have also been recently made using mass spectrometry as both a separation and a characterization technique.[1] Soft ionization techniques such as electrospray ionization (ESI)[2,3] and ultrahigh resolution and ultrahigh accuracy mass analyzers, typically Fourier transform ion cyclotron resonance mass spectrometry (FT-ICR MS),[4,5] have been successfully used in crude oil analysis. These techniques have contributed to the challenge of petroleum analysis via Petroleomic, which aims to provide comprehensive characterization of the organic and inorganic composition of petroleum and its derivatives and products.[6−10] FT-ICR MS has been the technique of choice for direct crude oil analysis due to the colossal complexity of its chemical composition and its ultrahigh resolution and accuracy, which enables the separation by mass of thousands of components in a single mass spectrum acquisition. Although less polar or nonpolar hydrocarbons predominate in crude oils, the ESI technique has been used extensively to investigate the polar species, detected basically as protonated or deprotonated molecules, which have been shown to function as proper indicators for many oil properties such as acidity, thermal evolution, treatment resistance, and biodegradation.[11−15]

Traditional geochemical evaluation of crude oils uses molecular composition of the saturated or aromatic hydrocarbon fractions and a series of biomarkers to infer about maturity, biodegradation, organic matter origin, and to perform oil−oil and oil−rock correlations.[16] The microbial crude oil alteration may however provide misleading predictions via biomarker analysis, for instance, due to modifications in molecules used for access thermal maturity.[16,17] Alternative biomarkers for biodegraded oils and new biodegradation parameters to evaluate biodegradation have therefore been proposed.[18−22] Biodegradation extent could also be inferred by *quasi*-stepwise scales,[16,23,24] but it is still quite difficult to achieve a global scheme because most oils are composed of a mixture of different oils or biodegraded through inconsistent patterns.[25]

For the analysis of the saturated hydrocarbons in crude oil, gas chromatography (GC) coupled to mass spectrometry (MS) has been the reference technique for many years.[16,26,27] More

Received: October 31, 2012
Revised: February 27, 2013
Published: March 1, 2013

Table 1. Codes, Previous Information, and Biodegradation Quantitative Parameters for the 16 Samples Studied

sample	code	25NH/H_{30}[a]	SA index[b]	A/C index[c]	classification[35,36]	main characteristics[35,36,d]
Cupiagua XU-34	Cp	n.d.	6.68%	0.08	non-biodegraded	*n*-Alks; no 25DH
Floreña C-3	Fl	n.d.	8.79%	1.10	non-biodegraded	*n*-Alks; no 25DH
Liria YB-3	Li	n.d.	2.50%	7.40	non-biodegraded	*n*-Alks; no 25DH
Pauto Sur B-1	PS	n.d.	0.82%	3.51	non-biodegraded	*n*-Alks; no 25DH
Trindad-15	Tr	n.d.	16.20%	0.36	non-biodegraded	*n*-Alks; no 25DH
El Palmar-2	EP	0.44	23.83%	0.21	biodegraded	low *n*-Alks; 25NH, 25DH
Buenos Aires W-18	BA-18	0.48	1.27%	0.86	mixture	*n*-Alks; low H, 25DH
Sardinas-2	S2	0.52	48.38%	0.18	non-biodegraded	*n*-Alks; 25NH, no 25DH
Tocaria-9	To	0.68	16.39%	0.21	mixture	*n*-Alks; 25NH, 25DH
Cusiana-1	C1	0.87	4.88%	1.36	mixture	*n*-Alks; low H, 25DH
Cusiana K-7	C7	1.01	6.18%	0.38	mixture	*n*-Alks; low H, 25DH
Buenos Aires GX-39	BA-39	1.15	5.61%	1.16	mixture	*n*-Alks; low H, 25DH
La Gloria-13-P	LG13	1.41	39.69%	0.06	biodegraded	low *n*-alk; High 25DH, 25NH
La Gloria-4	LG4	1.43	56.90%	0.09	biodegraded	low *n*-alk; high 25DH, 25NH
La Gloria norte-3	LG3	1.82	47.69%	0.04	biodegraded	low *n*-alk; high 25DH, 25NH
Rio Cusiana	RC		63.02%	0.12	biodegraded	no *n*-alks, no 25DH, 25NH

[a]From m/z 191 chromatogram peak areas of H_{29} 17α(*H*),21β(*H*)-25-*nor*-hopane (25NH) and H_{30} 17α(*H*),21β(*H*)-30-hopane. [b]Low DBE acids index, proposed in the text. [c]Modified acyclic:cyclic acids ratio previously proposed.[32] [d]*n*-Alks = *n*-alkanes; 25DH = 25 demethylated hopane series; 25NH = 25-*nor*-hopane; H = hopanes; n.d. = not detected.

recently, instrumentation developments brought up a new GC dimension, and now the 2D GC×GC technology offers a powerful tool for detailed analysis of the less polar components of crude oils,[28−30] but FT-ICR MS is being increasingly used as an alternative or to complement the organic geochemistry assessments via trends in polar components.[31] For instance, Pomerantz et al. used ESI FT-ICR MS focusing on the O_2 class to investigate reservoir connectivity,[32] based on the biodegradation index proposed by Kim et al.[33] Later, Hughey et al. used ESI FT-ICR MS to interrogate nitrogen, sulfur, and oxygen (NSO) compounds of both surface- and reservoir-biodegraded oils.[34] Naphthenic acids were also analyzed in crude oils by ESI FT-ICR MS to evaluate biodegradation[35] and naphthenic corrosion.[36]

Despite the well-established FT-ICR MS characterization of crude oil samples, few systematic studies have dealt with biodegradation markers or indexes in crude oils. Kim et al.[33] were the first to propose a biodegradation index based on O_2-profile, which was termed the A/C ratio (acyclic to cyclic naphthenic acids). This index is calculated from the sum of ion abundances of the acyclic (DBE = 1, Z = 0) O_2 species divided by the sum of ion abundances of the mono-, di-, and tricyclic acids (DBE = 2, 3, and 4; Z = 2, 4, and 6, respectively). The A/C ratio showed a good correlation with degree of biodegradation of some crude oils, but its broader applicability has not been demonstrated. In this study, using samples from crude oils from the Llanos Orientales basin, we propose the use of two indexes based on saturated acid ion abundance to predict biodegradation levels.

An alternative approach to process FT-ICR MS data to find diagnostic trends is via chemometric analysis.[37,38] Data mining techniques have been widely recognized as a valuable support to discovering significant patterns from MS data. A common procedure is to apply classic clustering schemes and equip them with the Euclidean distance. A universal and well-established clustering technique is principal component analysis (PCA),[39] which requires neither calibrants nor any assumptions about the samples. PCA is well understood and is used in industrial process monitoring and control situations.[40]

The present study has employed ESI FT-ICR MS in the negative ion mode focused on the O_2 class to analyze a series of samples from the Llanos Orientales Basin, Colombia. The aim was to use well-characterized samples as a reliable set to test the usefulness of the technique associated with PCA treatments for biodegradation classification. New approaches for classifying these samples according to biodegradation levels are proposed and compared.

EXPERIMENTAL SECTION

Samples. The samples studied in this work are from Llanos Orientales Basin − Colombia, and correspond to a subset of 16 samples studied previously using GC−MS.[41,42] These samples were chosen because the Llanos Orientales Basin oils have already been studied extensively and present a wide range of maturity and biodegradation with well-established values.[43] Details from the basin can be found elsewhere (Springer et al.[41] and references therein), whereas Table 1 displays the most relevant sample characteristics.

ESI(−) FT-ICR MS. Samples (approximately 4 mg) were dissolved in 10 mL of toluene, and then 0.5 mL of this solution was transferred to a 1 mL vial and diluted with 0.5 mL of methanol, containing 0.2% of ammonium hydroxide. Solvents and additives were of HPLC grade, purchased from Sigma-Aldrich, and used as received. General ESI conditions were as follows: capillary voltage of 3.10 kV, tube lens −100 V, and flow rate of 3 μL min^{-1}.

Ultrahigh resolution MS was performed with a Thermo Scientific 7.2 T electrospray ionization Fourier transform ion cyclotron resonance mass spectrometer (ThermoScientific, Bremen, Germany). A scan range of m/z 200−1000 was used, and 100 microscans were collected in each run. The average resolving power (R_p) was 400 000 at m/z 400, where R_p was calculated as $M/\Delta M_{50\%}$, that is, the m/z value divided by the peak width at 50% peak height. Time-domain data (ICR signal or transient signal) were acquired for 700 ms. The molecular weight distribution for each sample was first verified by LTQ analysis to ensure the validity of the molecular weight distribution based on FT-ICR MS.

Data Processing. For petroleomic information, mass spectra from FT-ICR were further processed with the PetroMS software specially designed for formula attribution and automatic recalibration for known homologous series from the measured m/z values of polar crude oil species.[44] For each spectrum, automated analysis was used to assign formulas to peaks with a signal-to-noise ratio (S/N) > 3. Allowed elements were ^{12}C, ^{1}H, ^{16}O, ^{14}N, ^{32}S, and ^{13}C. The maximum allowed

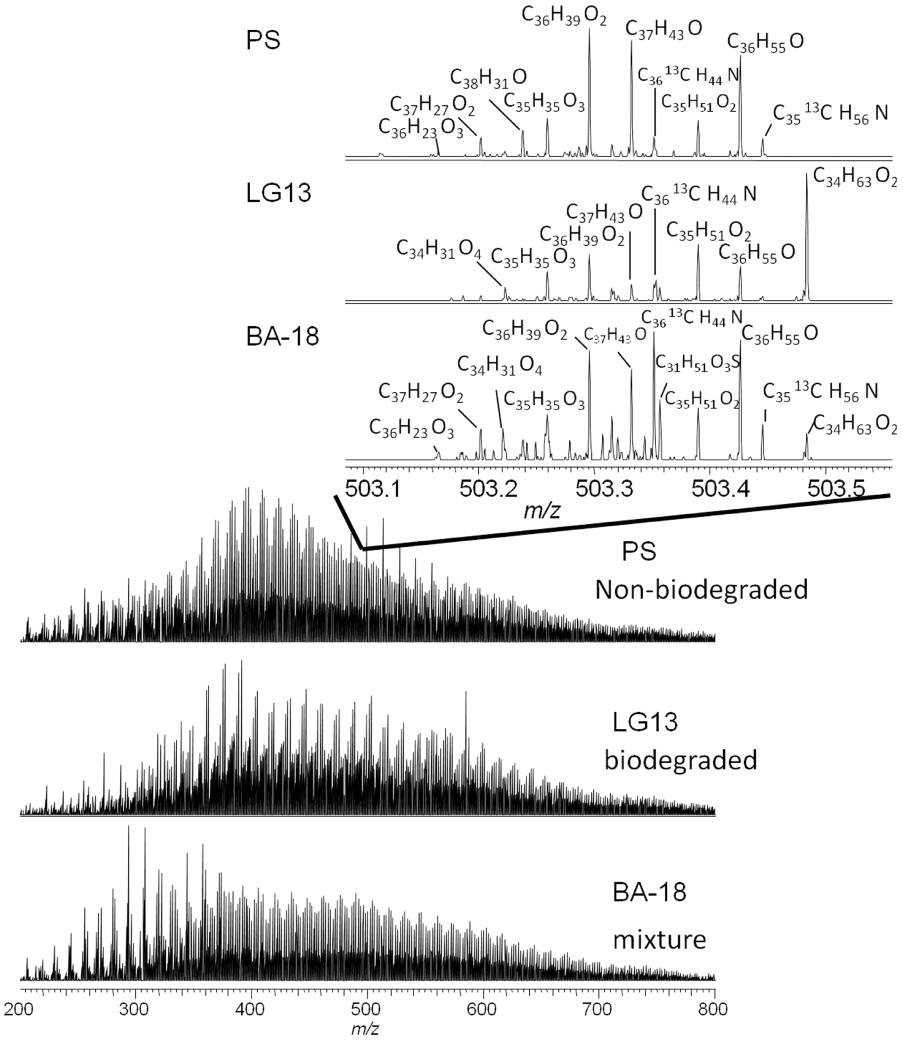

Figure 1. ESI(−) FT-ICR MS of non-biodegraded (PS), biodegraded (LG13), and mixture (BA-18) crude oils.

formula error was 1 ppm, and the mass limit for empirically assigning elemental formulas was 500 Da. Formulas above 500 Da were assigned through the detection of homologous series. If no chemical formula matched an m/z value within the allowed error, the peak was not included in the list of elemental formulas. For each elemental composition, $C_cH_hN_nO_oS_s$, the heteroatom class, type (double bond equivalents, DBE = the number of rings plus double bonds involving carbon), and carbon number, c, were tabulated for subsequent generation of heteroatom class relative abundance distributions and graphical DBE versus carbon number images.

Multivariate Analysis. To classify the crude oil samples, PCA was performed using the Pirouette software (version 3.11, Infometrix Inc., Woodinville, WA) from a matrix **X** (16, 1108), built using the relative intensity of 1108 different O_2 species, identified by PetroMS software.[44] Several preprocessing techniques and their combinations were tested. The best results were obtained from mean-center.

RESULTS AND DISCUSSION

Traditional Biomarker Analysis. Classical biomarker analyses via GC−MS were conducted to determine the degrees of biodegradation (Table 1). Biodegraded oils were so classified based on *n*-alkane peak low intensity in the gas chromatogram of the whole oil, the presence of demethylated hopanes (m/z 177), and the higher level of H_{29} 17α(*H*),21β(*H*)-25-*nor*-hopane to H_{30} 17α(*H*),21β(*H*)-hopane (25NH/H_{30}) ratio.[41,42] Non-biodegraded oils were so classified based on the distinct presence of *n*-alkane series in the gas chromatogram of the whole oil and the absence of H_{29} 17α(*H*),21β(*H*)-25-*nor*-hopane. Samples for which both H_{29} 17α(*H*),21β(*H*)-25-*nor*-hopane and the *n*-alkane homologues were found were classified as mixtures.[41,42] Other geochemical variables that might interfere with the following discussions (thermal maturity, fluid migration, lithology, etc.) were only partially addressed with this approach because they are difficult to detect and their effects on data are not clear.

Ultrahigh Resolution and Accuracy Mass Spectrometry. Figure 1 shows the broadband mass spectrum of representative crude oils of each class. Note that the spectra contain ∼1000−4000 peaks between m/z 200−800 (average m/z 420) with multiple mass spectral peaks at every nominal mass. In the present experiment, the average resolving power, $m/\Delta m_{50\%}$, in which $\Delta m_{50\%}$ is mass spectral peak full width at half-maximum peak height, is ∼400 000 for these crude oils. Because peaks are baseline-resolved, their m/z values may be determinate with very high accuracy, allowing for molecular assignment with low error. In fact, molecular formulas could be assigned to all 20 peaks at nominal mass of 503 Da with average error of ∼0.5 ppm (Figure 1).

ESI[45] in the negative ion mode typically favors the detection of acid species in their deprotonated forms $[M - H]^-$. For crude oils, this selectivity translates to the preferential

dx.doi.org/10.1021/ef301766r | Energy Fuels 2013, 27, 1277−1284

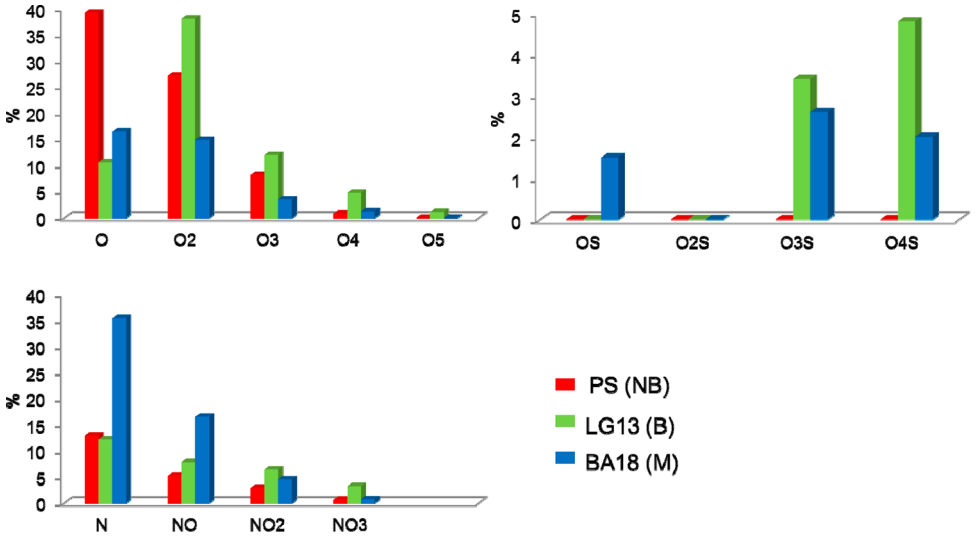

Figure 2. Class distribution changes in crude oils as revealed by ESI(−) FT-ICR MS.

ionization of OH > NH > SH containing compounds from the polar fraction. Figure 1 shows, for representative samples, mass spectrum segments of all three crude oils at nominal m/z 503, illustrating the compound classes found at odd masses, as well as the high complexity characteristic of petroleum mixtures. For BA-18 crude (Figure 1C), which is the most complex sample, 12 of 20 peaks (all with magnitude higher than 3σ of baseline noise) within 0.4 m/z range could be assigned molecular formulas of six classes: O, O_2, O_3, O_4, O_3S, ^{13}CN. The other two crudes, LG13 (Figure 1B) and PS (Figure 1A), exhibit five of six classes similar to those identified for BA-18 crude.

Figure 2 shows differences in percent relative abundances between the negative-ion heteroatomic class for representative non-biodegraded, mixture, and biodegraded crude oil samples. The diagrams of Figure 2 were calculated for oxygen-only containing classes, one for nitrogen-containing classes, and one for sulfur-containing classes. The relative abundances for each compound class are summed over all nominal masses, and then divided by the total relative abundance for all peaks. Although this approach does not take into account suppression effects (differences in ionization efficiencies within and between compound classes), or the effect of instrument parameters such as the time-of-flight effect, the approach is justified because similar mixtures are compared.

Oxygen-Only Containing Classes. Previous analyses of crude oils by ESI FT-ICR MS in the negative ion mode have shown that (1) the abundance of O_2-species is greater in biodegraded than non-biodegraded crude oils and (2) the abundance of O_2-species increases as the degree of biodegradation increases.[34] Carboxylic acids are known to be key intermediates during the aerobic and anaerobic metabolism of petroleum hydrocarbons. For example, bacterial degradation of *n*-alkanes involves the oxidation of the terminal methyl group with the formation of alcohols, and dehydrogenation of the alcohols via aldehydes to carboxylic acids. The carboxylic acids are in turn metabolized by the β-oxidation pathway.[46,47] Degradation of aromatic compound generally involves initial carboxylation followed by degradation to the respective aromatic acid, and then a series of hydrogenation steps to give the naphthenic acid, which possibly is a class of dead end metabolites.[48]

Figure 2 clearly shows that the O_2 class functions indeed as an effective biomarker class for crude oil degradation, because biodegradation substantially increases the relative abundance of this class in the polar fraction of the oil. These MS trends display also a direct correlation with geochemistry knowledge that tells that biodegradation turns hydrocarbons into organic acids. The LG13 biodegraded crude oil displays also the highest relative abundance in O_3, O_4, and O_5 classes, suggesting that this oil has undergone microbial degradation. On the contrary, the PS non-biodegraded oil has the uppermost relative abundance in O class, whereas the BA-18 crude oil displays relative abundances for oxygen-containing species between those of LG13 and PS crude oils. However, we expected that PS sample would display the lowest relative abundance of O_2 compounds with the BA-18 placed in the intermediate position, but this is not seen in Figure 2. Such results demonstrate the inadequacy of classifying stepwisely biodegraded samples using only trends in the O_2 class. As shown below, a detailed investigation of type distribution of O_2 class, carbon number distribution, and chemometric analysis is requested for proper classification of crude oils according to biodegradation levels using ESI(−) FT-ICR MS data.

Nitrogen- and Sulfur-Containing Classes. The N- and S-containing heteroatomic classes also are known to be major constituents of the polar fractions of crude oils. The N-class is known to translate mainly to pyrroles, carbazoles, and indoles. The NO_X-class (e.g., NO, NO_2, and NO_3) translates to furrolic, phenolic, and/or carboxylic analogues acids. From the ESI(−) FT-ICR MS, the BA-18 appears to have considerably more N-containing species than LG13 and PS crudes. The real composition is however likely different because ESI(−) efficiency increases as a function of acidity. Therefore, carboxylic acids ionize more efficiently than carbazoles, for instance. As evidenced by O-containing class bar graph (Figure 2), the LG13 has the O_2 class as the most abundant. The BA-18 has low O_x class content and high N_1 class content.

The NO_X (X = 2 and 3) classes appear in highest and lowest relative intensity in LG13 and PS crude oil, respectively. As pointed out earlier, the NO_X class may also encompass carboxylic acids and should be intermediate metabolites of biodegradation. The anaerobic degradation of alkyl-N-containing compounds produce alkylated phenols (e.g., NO class).[49]

dx.doi.org/10.1021/ef301766r | *Energy Fuels* 2013, 27, 1277−1284

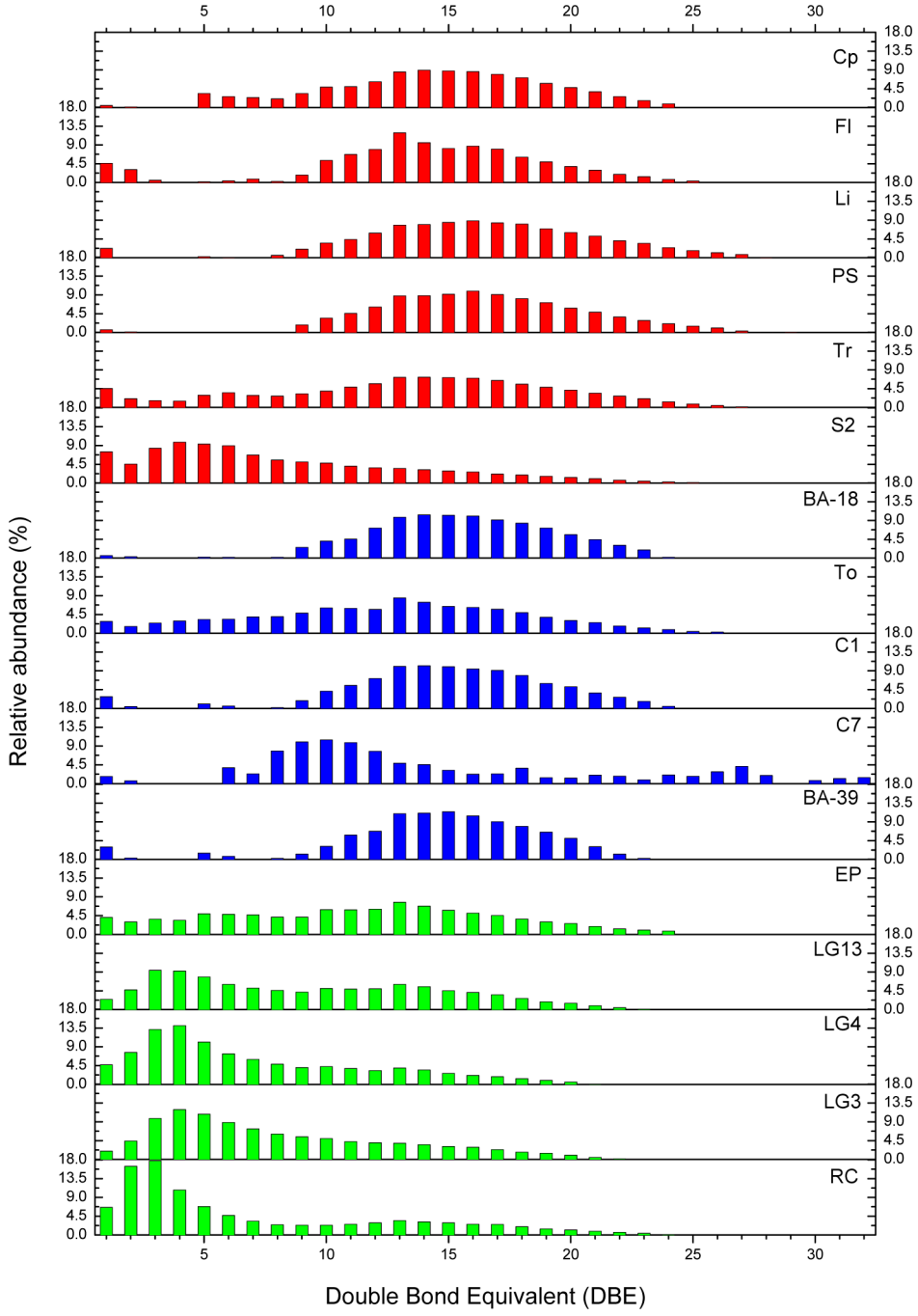

Figure 3. Double bond equivalents (DBE) distributions for oxygen-containing components (O_2) in the crude oils on the basis of ESI(−) FT-ICR MS. Red, blue, and green bars are from samples classified by GC−MS analysis as non-biodegraded, mixtures, and biodegraded samples, respectively.

However, the NO compounds produced could then be consumed by further biodegradation resulting in the conversion to NO_X products, which can occur under aerobic or anaerobic conditions. The LG13 crude oil has high NO_X content and, subsequently, higher biodegration level.

The S-containing molecules in crude oil have great geochemical relevance. Most sulfur in crude oils is introduced into the sediment early in diagenesis of petroleum formation (e.g., kerogen formation). The organic matter passes from aerobic to anaerobic to anoxic conditions. Ultimately, bio-organisms use sulfate as a terminal electron acceptor and produce H_2S as a byproduct. In the marine carbonate environment, iron is limited, leaving H_2S to react with functionalities in the organic molecules, either directly or through polysulfide intermediates. The S-containing compounds are of greatest molecular interest when comparing crude oil with varying degrees of biodegradation. For these compounds, relative abundances of Figure 2 directly and properly correlate with biodegradation degree of the oils. The LG13 biodegraded oil has the highest content of oxygen−sulfur-containing compounds followed by the BA-18 sample, classified as a mixture.

Biodegradation Information from Crude Oil Compositional Differences. As mentioned above, the ESI(−) FT-ICR MS approach is based on variations in relative abundances of polar biomarker classes identified by the unequivocal molecular

dx.doi.org/10.1021/ef301766r | *Energy Fuels* 2013, 27, 1277−1284

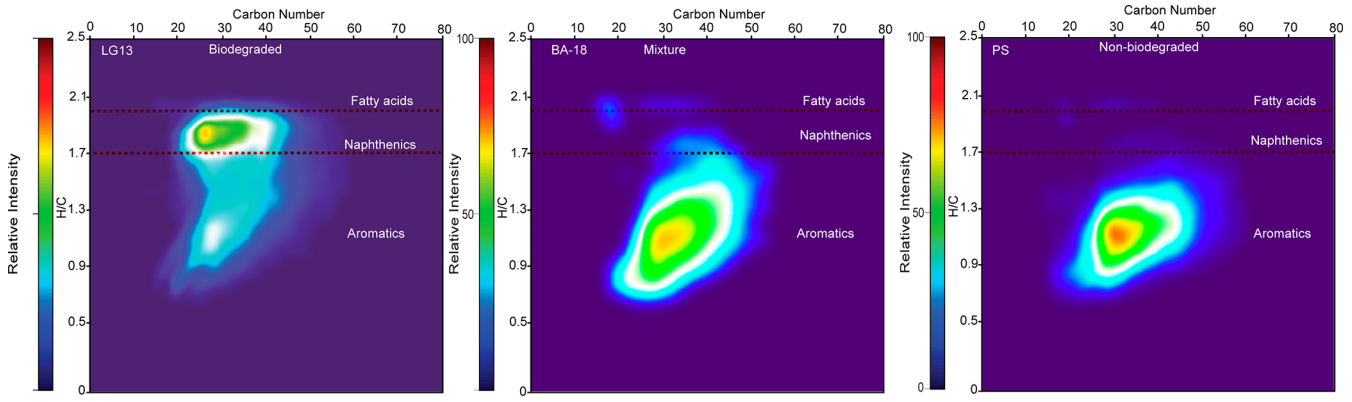

Figure 4. Graphs of H/C versus number of carbon of oxygen-containing components (O_2) for biodegraded (LG13), non-biodegraded (PS), and mixture (BA-18) crude oil.

formulas attributed to each ion in the spectra. Besides class, the formula also provides the number of carbons, the hydrogen deficiency as expressed by the DBE number, as well as the possible number of methylene groups (CH_2) with typically a rms mass error lower than 1.0 ppm. These trends are commonly displayed in the form of diagrams, which organize the huge amount of information furnished by ESI(−) FT-ICR MS.

Figure 3 shows an attempt to monitor changes in chemical composition as a function of biodegradation by visualizing the changes in relative abundances of the O_2 class (composed mainly of naphthenic acids) as a function of the DBE level. Note that, in general, biodegraded samples (green bars) display a typical shift to low DBE values, reaching their maximum intensity below DBE 5. The O_2 acids with DBE lower than 5 must display saturated chains and/or saturated rings, because aromatic acids should exhibit DBE equal or higher than 5. For nondegraded samples (red) and mixtures (blue), note that the most abundant O_2-species are those with DBE from 10 to 20. Notably, there are few exceptions to these behaviors. The EP sample has been previously classified as biodegraded but has the lowest abundance for acids with low DBE in this group. This sample also displays a low $25NH/H_{30}$ index, which is evidence that not only EP is a boundary member but also $25NH/H_{30}$ and the low DBE profile have an intrinsic correlation. Samples having profiles comparable to EP are both Tr (non-biodegraded) and To (mixture), having the intensities equally spread from DBE 1 to 25, with maximum near DBE 12. Clearly, the S2 sample also appears misclassified because it exhibits a DBE profile similar to that of biodegraded oils, similar to the LG3 sample, specifically. Sample C7 presented a distinguished composition profile, having a maximum between degraded and nondegraded samples values (DBE ∼9). Interestingly, C7 also presents considerable intensities over DBE 20, which was not seen for the other biodegraded samples. The similarity between Li and PS profiles is remarkable. The biodegraded samples RC, LG3, LG4, and LG1 show that extensive biodegradation is visible in low DBE values, even though suitable shape differences are found on the RC sample.

Figure 4 displays plots of the H/C ratios versus carbon number for one typical example of each class. H/C ratio is an indirect measurement of aromaticity for a given molecular formula. It is again clearly highlighted in such plots that enhanced biodegradation (left as compared to right plot) increases the H/C ratios, whereas the maximum in carbon number remains practically the same. The mixture (center plot) shows, as expected, an average trend. Two possible scenarios might explain the increasing H/C values for biodegraded oils. First, aromatic acids are being hydrogenated during biodegradation; second, new saturated acid species are being formed, decreasing the relative abundance of low H/C species, as observed. Both hypotheses are corroborated by recent discussions, which have suggested that anaerobic bacteria present in water droplets might be trapped in bacterial biofilms at the water/oil interface, producing oxygen by reducing nitrates and perchlorates during anaerobic life cycles. The biofilm would therefore act as an oxygen sponge that could have either high or low oxygen content. Anaerobic biodegradation activity would then slowly decrease with increasing oxygen content, and the degradation activity would be taken over by the aerobic consortium, consequently consuming the stored oxygen.[50] The generation of new saturated acid species not only would explain the increase in H/C ratios but also would corroborate with the microbial preference to the saturates, as it has been long observed and explained in traditional biodegradation scales.[16,23]

In general, samples behaved slightly different from previously observed[33] regarding to their saturated acid distribution. First, the devised biodegradation parameter[33] from the ratio between the acyclic and cyclic O_2 species (A/C index) has received different interpretations of its original formula, being calculated sometimes as the ratio between DBE 1 and DBE 2−4 or as DBE 1 over DBE 3−5.[32,34] Despite the fact that Hughey et al.[34] had problems on classification, specifically when compared to a typical biodegradation rank,[16] the A/C index has provided proper insights of biodegradation levels, because good relationships between the A/C index measured by GC−MS and the total acid number of oil samples were attained.[51] In Llanos Orientales Basin samples shown in this study, however, the A/C index failed to provide proper order on biodegradation levels.

A good overall picture of the biodegradation levels could however be obtained when the A/C index was slightly modified and coupled to a new parameter proposed herein. This new parameter is given by the sum of relative abundances of DBE 1−6 for the class O_2 (SA index − saturated acid index), and is based on the observed effects of microbial activity, which generates low DBE O_2 species shifting the intensities toward these values. DBE values of 5−6 might also have contribution from acidic aromatic species; however, their inclusion in the formula is crucial to capture the effect of biodegradation on 4-

dx.doi.org/10.1021/ef301766r | Energy Fuels 2013, 27, 1277−1284

ring steroids and 5-ring hopanes (and related) molecules. Modifications on A/C index were also made to take 4- and 5-ring naphthenic acids into account, calculating the ratio between DBE 1 and DBE 2−6.[52] In this sense, the SA index looks at the biodegradation scheme from the produced compounds rather than those consumed, as established in typical biodegradation rank.

Figure 5 shows a plot for sample behaviors using both indexes. The SA threshold value within these samples was 20%;

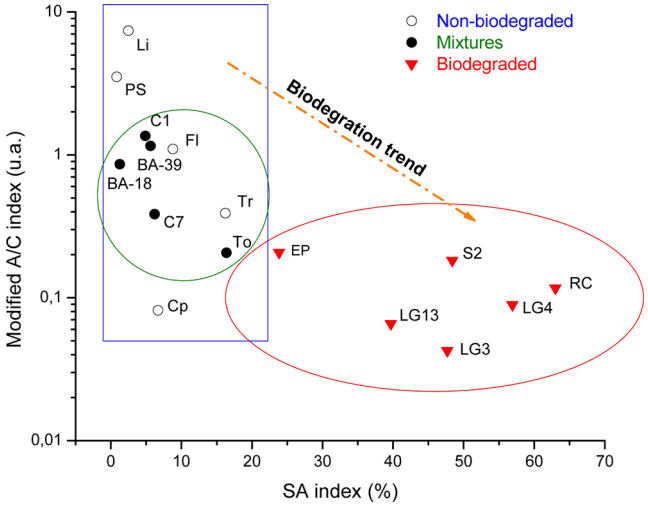

Figure 5. Sample behavior facing both SA and A/C indexes. An almost exponential trend can be inferred from sample PS to sample RC, the end members.

that is, samples with SA index >20% were considered biodegraded. As discussed previously, EP has a boundary characteristic similar to Tr (non-biodegraded) and To, all of them found close to each other in the center of the figure. This is the most intriguing sample subset, because their chromatographic characteristics (Table 1) are significantly different. Regarding this continuous classification based on biodegradation, end-members are promptly identified in Figure 5; clearly Li is non-biodegraded and LG4 is biodegraded. Non-biodegraded crudes were placed on the mixture area, which likely indicates a low content of biodegraded material.

Another way to classify samples in terms of biodegradation from FT-ICR MS data on the O_2 class would be via the application of PCA. As Figure 6 shows, PCA was quite effective at placing the samples into three quite well-defined and correctly assigned groups: biodegraded, non-biodegraded, and mixtures. The loadings in Figure 6 reveal, as seen in Figures 3 and 4, that lower DBE compounds (fatty and naphthenic acids) and higher carbon numbers are the main constituents responsible for the grouping of the biodegraded oils. The PCA of Figure 6 also seems to provide an indication of degradation level: the LG3 and S2 samples are quite apart in the biodegraded group due to their high level of biodegradation, as was also indicated by Figure 3. Note that the Fl sample, which has been previously classified as a non-biodegraded sample, was classified in Figure 6 as a mixture. In Figure 5, Fl also appears close to samples BA-39, BA-18, and C1, previously classified as mixtures.

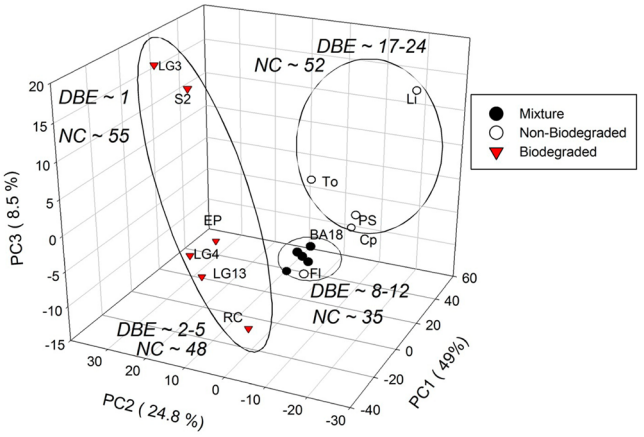

Figure 6. PCA from the 15 crude oil samples for the ESI(−) FT-ICR MS data. NC is the number of carbon atoms.

CONCLUSIONS

The ESI(−) FT-ICR MS approach focused on the O_2 class in combination with clustering methods such as PCA seems to offer therefore an effective approach to classify biodegraded and non-biodegraded oils, and their mixtures. These findings are complementary to the traditional GC−MS biomarker analysis and can allow new insights in crude oil analysis.

A plot using both A/C and SA indexes was found useful to categorize samples and to quantitate the biodegradation extent.

AUTHOR INFORMATION

Corresponding Author

*E-mail: bonigontijo@yahoo.com.br (B.G.V.); renzocsilva@gmail.com (R.C.S.); eberlin@iqm.unicamp.br (M.N.E.); debora@iq.ufrj.br (D.A.A.).

Notes

The authors declare no competing financial interest.

ACKNOWLEDGMENTS

We thank CAPES, FAPERJ, and CNPq (Brazilian research councils) for fellowships and FAPESP, FAPERJ, FUJB, CAPES, CNPq, and Petrobras S/A for financial support.

REFERENCES

(1) Rodgers, R. P.; McKenna, A. M. *Anal. Chem.* **2011**, *83*, 4665−4687.
(2) Whitehouse, C. M.; Dreyer, R. N.; Yamashita, M.; Fenn, J. B. *Anal. Chem.* **1985**, *57*, 675−679.
(3) Gaskell, S. J. *J. Mass Spectrom.* **1997**, *32*, 677−688.
(4) Comisarow, M. B.; Marshall, A. G. *Chem. Phys. Lett.* **1974**, *25*, 282−283.
(5) Marshall, A. G.; Hendrickson, C. L.; Jackson, G. S. *Mass Spectrom. Rev.* **1998**, *17*, 1−35.
(6) Marshall, A. G.; Rodgers, R. P. *Proc. Natl. Acad. Sci. U.S.A.* **2008**, *105*, 18090−18095.
(7) Hsu, C. S.; Hendrickson, C. L.; Rodgers, R. P.; McKenna, A. M.; Marshall, A. G. *J. Mass Spectrom.* **2011**, *46*, 337−343.
(8) Hur, M.; Yeo, I.; Park, E.; Kim, Y. H.; Yoo, J.; Kim, E.; No, M.-h.; Koh, J.; Kim, S. *Anal. Chem.* **2010**, *82*, 211−218.
(9) Kim, S.; Rodgers, R. P.; Marshall, A. G. *Int. J. Mass Spectrom.* **2006**, *251*, 260−265.
(10) Liu, P.; Shi, Q.; Chung, K. H.; Zhang, Y.; Pan, N.; Zhao, S.; Xu, C. *Energy Fuels* **2010**, *24*, 5089−5096.

(11) Mapolelo, M. M.; Rodgers, R. P.; Blakney, G. T.; Yen, A. T.; Asomaning, S.; Marshall, A. G. *Int. J. Mass Spectrom.* **2011**, *300*, 149−157.
(12) Hughey, C. A.; Rodgers, R. P.; Marshall, A. G.; Walters, C. C.; Qian, K.; Mankiewicz, P. *Org. Geochem.* **2004**, *35*, 863−880.
(13) Smith, D. F.; Rodgers, R. P.; Rahimi, P.; Teclemariam, A.; Marshall, A. G. *Energy Fuels* **2009**, *23*, 314−319.
(14) Wu, Z.; Rodgers, R. P.; Marshall, A. G.; Strohm, J. J.; Song, C. *Energy Fuels* **2005**, *19*, 1072−1077.
(15) Wang, J.; Zhang, X.; Li, G. *Chemosphere* **2011**, *85*, 609−615.
(16) Peters, K. E.; Walters, C. C.; Moldowan, J. M. *The Biomarker Guide*; Cambridge University Press: New York, 2005.
(17) Bao, J. P.; Zhu, C. S. *Sci. China, Ser. D* **2009**, *52*, 42−50.
(18) Elias, R.; Vieth, A.; Riva, A.; Horsfield, B.; Wilkes, H. *Org. Geochem.* **2007**, *38*, 2111−2130.
(19) De Lima, S. G.; Steffen, R. A.; Reis, F. A. M.; Koike, L.; Santos Neto, E. V.; Cerqueira, J. R.; Lopes, J. A. D. *Org. Geochem.* **2010**, *41*, 325−339.
(20) Asif, M.; Grice, K.; Fazeelat, T. *Org. Geochem.* **2009**, *40*, 301−311.
(21) Grice, K.; Alexander, R.; Kagi, R. I. *Org. Geochem.* **2000**, *31*, 67−73.
(22) Silva, T. F.; Azevedo, D. A.; Rangel, M. D.; Fontes, R. A.; Aquino Neto, F. R. *Org. Geochem.* **2008**, *39*, 1249−1257.
(23) Larter, S.; Huang, H.; Adams, J.; Bennett, B.; Snowdon, L. R. *Org. Geochem.* **2012**, *45*, 66−76.
(24) Wenger, L. M.; Davis, C. L.; Isaksen, G. H. *SPE Reserv. Eval. Eng.* **2002**, *5*, 375−383.
(25) Bennett, B.; Larter, S. R. *Org. Geochem.* **2008**, *39*, 1222−1228.
(26) Hunt, J. M.; Philp, R. P.; Kvenvolden, K. A. *Org. Geochem.* **2002**, *33*, 1025−1052.
(27) Wang, Z.; Stout, S. A.; Fingas, M. *Environ. Forensics* **2006**, *7*, 105−146.
(28) Frysinger, G. S.; Gaines, R. B. *J. Sep. Sci.* **2001**, *24*, 87−96.
(29) Oliveira, C. R.; Ferreira, A. A.; Oliveira, C. J. F.; Azevedo, D. A.; Santos Neto, E. V.; Aquino Neto, F. R. *Org. Geochem.* **2012**, *46*, 154−164.
(30) Aguiar, A.; Aguiar, H. G. M.; Azevedo, D. A.; Aquino Neto, F. R. *Energy Fuels* **2011**, *25*, 1060−1065.
(31) Ávila, B. M. F.; Vaz, B. G.; Pereira, R.; Gomes, A. O.; Pereira, R. C. L.; Corilo, Y. E.; Simas, R. C.; Lopes Nascimento, H. D.; Eberlin, M. N.; Azevedo, D. A. *Energy Fuels* **2012**, *26*, 5069−5079.
(32) Pomerantz, A. E.; Ventura, G. T.; McKenna, A. M.; Cañas, J. A.; Auman, J.; Koerner, K.; Curry, D.; Nelson, R. K.; Reddy, C. M.; Rodgers, R. P.; Marshall, A. G.; Peters, K. E.; Mullins, O. C. *Org. Geochem.* **2010**, *41*, 812−821.
(33) Kim, S.; Stanford, L. A.; Rodgers, R. P.; Marshall, A. G.; Walters, C. C.; Qian, K.; Wenger, L. M.; Mankiewicz, P. *Org. Geochem.* **2005**, *36*, 1117−1134.
(34) Hughey, C. A.; Galasso, S. A.; Zumberge, J. E. *Fuel* **2007**, *86*, 758−768.
(35) Hughey, C. A.; Minardi, C. S.; Galasso-Roth, S. A.; Paspalof, G. B.; Mapolelo, M. M.; Rodgers, R. P.; Marshall, A. G.; Ruderman, D. L. *Rapid Commun. Mass Spectrom.* **2008**, *22*, 3968−3976.
(36) Barrow, M. P.; McDonnell, L. A.; Feng, X.; Walker, J.; Derrick, P. J. *Anal. Chem.* **2003**, *75*, 860−866.
(37) Vaz, B. G.; Abdelnur, P. V.; Rocha, W. F R.; Gomes, A. O.; Pereira, R. C. L. *Energy Fuels*, DOI: 10.1021/ef301515y.
(38) Chiaberge, S.; Fiorani, T.; Savoini, A.; Bionda, A.; Ramello, S.; Pastori, M.; Cesti, P. *Fuel Process. Technol.* **2013**, *106*, 181−185.
(39) Wold, S.; Esbensen, K. H.; Geladi, P. *Chemom. Intell. Lab. Syst.* **1987**, *2*, 37−52.
(40) Gurden, S. P.; Martin, E. B.; Morris, A. J. *Chemom. Intell. Lab. Syst.* **1998**, *44*, 319−330.
(41) Springer, M. V.; Garcia, D. F.; Gonçalves, F. T. T.; Landau, L.; Azevedo, D. A. *Org. Geochem.* **2010**, *41*, 1013−1018.
(42) Springer, M. V. Caracterização de Biomarcadores e Diamantoides em Amostras de Óleos da Bacia Llanos Orientales, Colômbia. M.Sc. Dissertation, Federal University of Rio de Janeiro, Rio de Janeiro, Brazil, 2007.
(43) Bautista, D. F. G. Estudo dos Sistemas Petrolíferos no Setor Central da Bacia dos "Llanos Orientales", Colômbia. Um Modelo para Explicar as Mudanças na Qualidade do Petróleo. Ph.D. Thesis, Federal University of Rio de Janeiro, Rio de Janeiro, Brazil, 2008.
(44) Corilo, Y. E.; Vaz, B. G.; Simas, R. C.; Lopes Nascimento, H. D.; Klitzke, C. F.; Pereira, R. C. L.; Bastos, W. L.; Santos Neto, E. V.; Rodgers, R. P.; Eberlin, M. N. *Anal. Chem.* **2010**, *82*, 3990−3996.
(45) Fenn, J. B.; Mann, M.; Meng, C. K.; Wong, S. F.; Whitehouse, C. M. *Science* **1989**, *246*, 64−71.
(46) Singer, M. E.; Finnerty, W. R. Microbial Metabolism of Straight-Chain and Branched Alkanes. In *Petroleum Microbiology*; Atlas, R. M., Ed.; Macmillan Publishing: New York, 1984; pp 1−60.
(47) Watkinson, R. J.; Morgan, P. *Biodegradation* **1990**, *1*, 79−92.
(48) Aitken, C. M.; Jones, D. M.; Larter, S. R. *Nature* **2004**, *431*, 291−294.
(49) Meredith, W.; Kelland, S.-J.; Jones, D. M. *Org. Geochem.* **2000**, *31*, 1059−1073.
(50) da Cruz, G. F.; Santos Neto, E. V.; Marsaioli, A. J. *Org. Geochem.* **2008**, *39*, 1204−1209.
(51) Fafet, A.; Kergall, F.; da Silva, M.; Behar, F. *Org. Geochem.* **2008**, *39*, 1235−1242.
(52) Liao, Y.; Shi, Q.; Hsu, C. S.; Pan, Y.; Zhang, Y. *Org. Geochem.* **2012**, *47*, 51−65.